Conformational Behavior and Magnetic Properties of a Nitroxide Amino Acid Derivative in Vacuo and in Aqueous Solution

Maddalena D'Amore, Roberto Improta,† and Vincenzo Barone*

Contribution from Dipartimento di Chimica, Universita Federico II, Complesso Universitario Monte S.Angelo, via Cintia, I-80126 Napoli, Italy

Received: February 11, 2003; In Final Form: May 19, 2003

The conformational behavior and magnetic properties of the α-acetylamino, *N*′-methylamide derivative of TOAC (4-amino-2,2,6.6-tetramethylpiperidine-1-oxyl-4-carboxylic acid) have been investigated in vacuo and in aqueous solution by an integrated computational approach including density functional, post-Hartree−Fock, and continuum solvent models. According to our computations, piperidine rings with an equatorial placement of the nitroxide moiety are more stable by about 1 kcal/mol than their axial counterparts both in vacuo and in aqueous solution. With respect to natural residues, TOAC shows a marked preference for helical conformers, which is further enhanced by polar solvents. A comparison with other C^{α}-tetrasubstituted residues points out the difference between cyclic and open-chain substituents. The nitrogen isotropic hyperfine coupling constants (A_N) of folded TOAC conformers are similar to those of other nitroxides involving six-membered rings and are well reproduced by a composite QM/QM/PCM model. The A_N values of extended TOAC conformers are significantly lower because of the constrained nearly planar structure of the piperidine ring.

Introduction

In the last few years, organic free radicals, especially nitroxides, have been largely exploited as magnetic probes or labels in the study of macromolecular systems by means of electron spin resonance (ESR) spectroscopy. The particularly interesting spin label 4-amino-2,2,6,6-tetramethylpiperidine-1-oxyl-4-carboxylic acid (hereafter, TOAC) is shown in Figure 1. This radical is stable under ordinary conditions, has a well-localized unpaired electron, and can enter into polypeptides or proteins, replacing natural amino acids and providing useful conformational information through well-established magneto-structural relationships. TOAC was first synthesized more than 3 decades ago[1] and was introduced into peptide chemistry about 15 years later.[2] A favorable property of TOAC over other spin-labeled amino acids is that rotation about side-chain bonds is hampered by the incorporation of the nitroxide nitrogen, C^{α}, C^{β}, and C^{γ} atoms into a cyclic moiety.[3−5]

TOAC is able to induce a dramatic quenching of suitably designed, fluorescence-labeled peptides[6,7] and is characterized by a weak ($\epsilon = 5-20$) adsorption band in the visible spectral region ($\lambda = 420-450$ nm), assigned to the $n \rightarrow \pi^*$ transition of the nitroxide chromofore, which may become optically active in a chiral peptide and be detected by CD.[8] Furthermore, it is able to undergo a reversible, nitroxide-based redox process that can be monitored by cyclic voltammetry and gives derivatives and peptides of extremely high crystallinity, whose structures have been characterized by X-ray diffraction.[9]

From a structural point of view, TOAC belongs to the family of conformationally constrained C^{α}-tetrasubstituted α-amino acids whose most widely investigated member is α-aminoisobutyric acid (Aib). Incorporating this class of residues into peptide chains provides a means of restricting the available range of backbone conformations.[10−14] In particular, it is well known that Aib strongly stabilizes $3_{10}/\alpha$ helical structures, and more recent studies have also shown that 1-aminocyclohexane-1-carboxylic acid (Ac_6c) has similar characteristics.

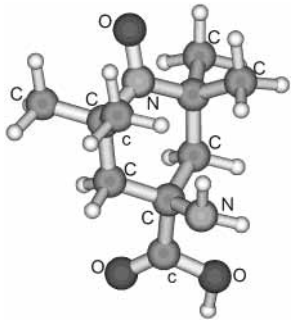

Figure 1. TOAC structure.

Crystallographic characterization of the geometry and conformation of TOAC in simple derivatives and short alanine (Ala) polypeptides[7,15] established a marked stereochemical rigidity of the peptide backbone, with a significant increase in helix stability and an inhibition of the unfolding of water-soluble Ala-rich sequences at elevated temperature.

TOAC is thus expected to become important in designing stereochemically restricted analogues of bioactive peptides containing a valuable spectroscopic probe.[16]

Because the magnitude of the nitrogen isotropic hyperfine coupling constant (hcc, A_N) of nitroxides depends remarkably on the features (mainly the polarity) of their environment, TOAC is indeed an ideal probe of the medium in which it is embedded, giving valuable information on the polarity, the hydrogen bonding power, and the pH of the solvent and on the proximity to other free radicals or charged species and so on. Furthermore, the line widths of the ESR spectra (and the effective rotational correlation time τ) are controlled by the rotational and lateral diffusion of the nitroxide, which is related, in turn, to the viscosity and the amount of order in and the temperature of the

* Corresponding author. E-mail: baronev@unina.it.
† Permanent address: Istituto di Biostrutture e Bioimmagini−CNR, via Mezzocannone 6, I-80134 Naples, Italy.

10.1021/jp030188j CCC: $25.00
Published on Web 07/22/2003

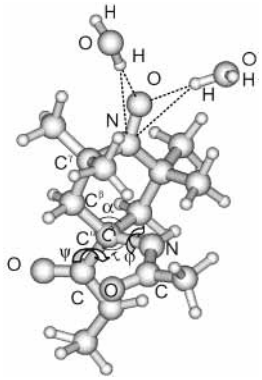

Figure 2. Definition of dihedral and bond angles for the TOAC dipeptide analogue. Two explicit water molecules are also represented.

spin−probe environment. Of course, isotropic hyperfine coupling constants critically depend on conformational characteristics.

TOAC incorporation into peptide sequences also provides spectroscopic ESR signatures that are useful in determining peptide geometry. TOAC double-labeled peptides were sinthesized; biradical *J* coupling and dipolar interactions between different TOAC residues within a peptide were used to determine peptide geometry as a function of the solvent[15] and to distinguish clearly between 3_{10} and α helices.

This situation prompted us to undertake a systematic quantum mechanical (QM) study of the structure and spectroscopic properties of TOAC and TOAC-labeled systems both in the gas phase and in aqueous solution. As a starting point, we have chosen the α-acetylamino-TOAC-*N*′-methylamide shown in Figure 2, which will be referred to as the TOAC dipeptide analogue (TOACDA).

It is now well established that computational models based on density functional theory (DFT) are particularly suitable for the analysis of the structure and magnetic properties of open-shell species.[18] The potential of DFT methods in the study of free radicals has been fully appreciated for nitroxides, which, being stable under ordinary conditions, allow a thorough comparison between experiments and computations.[19] Calculations have been performed on five-membered ring nitroxides,[20] which have been used mostly as spin probes, as well as on six-membered ring analogues.[21]

These calculations show bond lengths close to the corresponding experimental values and good agreement between calculated and experimental bond angles. Because the value of A_N critically depends on the competition between pyramidal and planar geometry around the nitrogen atom, it is worth noting that all of the calculated out-of-plane angles are close to their experimental counterparts.

In the present context, the backbone conformation could have some effect on the puckering of the piperidine ring, which might in turn tune the A_N value. These effects can be effectively studied by proper QM computations, which also allow us to characterize high-energy conformers.

DFT methods including a fraction of the Hartree−Fock (HF) exchange (hybrid functionals) often provide a better description of the structures and physicochemical properties of molecules of biological interest.[22] Therefore, we have decided to compare in the present study a conventional functional (PBE)[23] and its hybrid counterpart (PBE0).[24]

Contrary to the general situation, the ESR couplings of nitroxide nitrogens obtained by density functional methods (irrespective of the specific functional) are significantly underestimated with respect to experiment.[19−21] As a consequence we have exploited the combined DFT/post-HF approach described in the following text.

Computational Aspects

A development version of the Gaussian package[25] was used for the entire study. Post Hartree−Fock computations have been performed by the quadratic configuration model including single and double excitations (QCISD)[26] and using the basis set developed by Chipman to compute magnetic properties.[27]

DFT calculations were carried out at the PBE level using the standard 6-31G(d) basis set and at the PBE0 level using both 6-31G(d) and 6-31+G(d,p) basis sets.[26,28]

We recall that PBE0 is a parameter-free hybrid HF/DFT method rooted in the adiabatic connection formula and based on fourth-order perturbation theory:[24]

$$E^{\mathrm{PBE0}} = E_{\mathrm{X}}^{\mathrm{PBE}} + E_{\mathrm{C}}^{\mathrm{PBE}} + \frac{1}{4}(E_{\mathrm{X}}^{\mathrm{HF}} - E_{\mathrm{X}}^{\mathrm{PBE}}) \qquad (1)$$

where E_X^{HF} is the HF exchange and E_X^{PBE} and E_C^{PBE} are the exchange and correlation density functionals proposed by Perdew, Burke, and Ernzerhof (PBE), respectively.[23]

For any magnetic nucleus, A_N is given by[29]

$$A_{\mathrm{N}} = \frac{8}{3}\pi g_{\mathrm{n}} g_{\mathrm{e}} \mu_{\mathrm{n}} \mu_{\mathrm{e}} \rho_{\mathrm{S}}(r_{\mathrm{N}}) \qquad (2)$$

where $\rho_S(r_N)$ is the electron spin density at the nucleus, and μ_n and g_n are the nuclear magneton and nuclear *g* factor, respectively. The term g_e is the *g* value for the electron (in the present work, $g_e = 2.0$), and μ_e is the Bohr magneton.

DFT methods are generally very effective for the evaluation of magnetic properties, providing isotropic hyperfine coupling constants in good agreement with their experimental counterparts.[18] However, the A_N of nitroxides is underestimated by DFT calculations, but coupled cluster (CC) and quadratic configuration interaction (QCISD) methods provide accurate estimates for this observable.[30]

Although the reliability of PBE0 geometries allows us to use the QCISD method only for single-point energy and propriety evaluations, even these computations become prohibitive for large systems. To conjugate accuracy and computational feasibility, A_N calculations have been performed on geometries optimized at the PBE0/6-31G(d) level with the following combined approach:

$$A_{\mathrm{N}} = A_{\mathrm{N}}^{\mathrm{PBE0}}(\mathrm{real}) + [A_{\mathrm{N}}^{\mathrm{QCISD}}(\mathrm{model}) - A_{\mathrm{N}}^{\mathrm{PBE0}}(\mathrm{model})] + A_{\mathrm{N}}^{\mathrm{PBE0}}(\mathrm{vibr}) \qquad (3)$$

where the superscript denotes the level of calculations, "real" refers to the whole amino acid derivative (including, when needed, explicit solvent molecules and bulk solvent effects), and the subscript "model" refers to a dimethyl nitroxide molecule in vacuo whose geometry is frozen to that assumed by the C_2−NO moiety in the real nitroxide. Methyl hydrogens are added following the standard recipe of ONIOM methods.[31] Actually, the only difference between our procedure and a conventional ONIOM calculation is the use of PBE0 geometries also for the model system. The last term of eq 3 refers to vibrational averaging effects induced by the out-of-plane motion of the nitroxide moiety. However, contrary to planar or quasi-planar nitroxide systems,[20] vibrational averaging effects are essentially negligible for piperidine rings.[21]

Bulk solvent effects on the structure and magnetic properties have been taken into account by our most recent implementation

of the polarizable continuum model (PCM).[32] In this method, the solvent is represented by an infinite dielectric medium characterized by the relative dielectric constant of the bulk (78.39 for H_2O at 25 °C and 1 atm). A molecule-shaped cavity contains the system under study (the solute) and separates it from the surrounding solvent. The cavity including the molecule, defined in terms of interlocking spheres centered on nonhydrogen atoms, is built by a new version of the Gepol procedure[33] using UAHF atomic radii.[34] The free energy of solvation (ΔG_{solv}) includes electrostatic, dispersion/repulsion,[35] and cavitation[36] contributions. Note that, in the current implementation, only electrostatic interactions are described by a quantum mechanical operator and have a direct effect on computed properties, even in the absence of geometry modifications.

In aqueous solution, it is also necessary to take into proper account the interactions between the nitroxide moiety and specific solvent molecules. The simultaneous inclusion of the bulk effect and of specific interactions can be modeled by considering adducts formed by the nitroxides and two water molecules, whose disposition is shown in Figure 2.

Following the analysis introduced by Cremer and Pople,[37] ring puckerings have been described in terms of the displacements (z_i) of the atoms from the average plane of the ring. For six-membered rings, there are three puckering degrees of freedom described by the "spherical polar set" (Q, θ, ϕ), where Q is the total puckering amplitude and the "distortion type" is specified by two angular variables θ ($0 \le \theta \le \pi$) and ϕ. This cooordinate system allows us to map all types of puckering for a given amplitude (Q) on the surface of a sphere. In particular, the polar position ($\theta = 0$ or 180°, $\phi = 0°$) corresponds to a chair conformation (C); the position on the equator of the sphere ($\theta = 90°$, $\phi = 90°$) is a twist-boat (TB) conformation, and the special boat conformation (B) is defined by $\theta = 0°$, $\phi = 0°$. The conformation characterized by a specific triplet of puckering coordinates can thus be described as a mixture of C, TB, and T structures with well-defined percentages.

Results and Discussions

The backbone arrangement of peptides depends mainly on the φ and ψ torsional angles. With reference to staggered conformations around each dihedral angle, the following five regions can be defined in the (φ, ψ) subspace (the so-called Ramachandran map): α ($\varphi \approx \pm 60°$, $\psi \approx \pm 60°$), β ($\varphi \approx 180°$, $\psi \approx 180°$), γ ($\varphi \approx \pm 60°$, $\psi \approx \mp 60°$), δ ($\varphi \approx 180°$, $\psi \approx \pm 60°$), ϵ ($\varphi \approx \pm 60°$, $\psi \approx 180°$). TOAC is not chiral, so we do not have enantiomeric pairs (L and R) for each structure; however, the number of possible minima is doubled by taking into account that the α-amino group can occupy either an equatorial (hereafter, eq) or an axial (hereafter, ax) position in the piperidine cycle.

Conformational Behavior. Geometrical parameters issuing from PBE/6-31g(d) optimizations are very close to their PBE0/6-31G(d) counterparts, and the same applies to the relative stabilities of different isomers (Tables 1 and 2). Furthermore, the inclusion of diffuse functions on heavy atoms and of polarization functions on hydrogens (6-31+G(d,p) basis set) has only a negligible effect on relative stabilities (Table 2). As a consequence, we will explicitly refer to PBE0/6-31G(d) results in the following text.

A comparison of our optimized geometries with the available experimental data[13,36] shows remarkable agreement concerning both bond lengths and valence angles (Figure 3).

As usual for dipeptide analogues in the gas phase, the absolute energy minimum falls in the γ region, its extra stability being related to the formation of an intramolecular hydrogen bond between carbonyl [$CO_{(i-1)}$] and amino [$NH_{(i+1)}$] groups that is quite strong. However, the β structure, exhibiting a distorted NH−CO hydrogen bond, is much less stable than in natural peptides (5−7 kcal/mol with respect to typical values of less than 1 kcal/mol) because of the constraints induced by the presence of the piperidine ring. For instance, in the β structure, the most stable chair ring arrangement would bring a hydrogen atom of the CH_2 group in the piperidine cycle too close to the oxygen atom of CO in the backbone. The issuing ring distortion leads to a significant energetic penalty. As a result, in α and γ structures, the piperidine ring is close to an ideal chair puckering,

TABLE 1: Relative Stabilities (kcal/mol) and Selected Geometrical Parameters of the TOACDA Conformers Obtained at the PBE/6-31g(d) Level

	φ (deg)	ψ (deg)	α (deg)	τ (deg)	ΔE
		Equatorial α-Amino Group			
α	−72.2	−16.0	108.0	111.6	3.4
β	145.3	−151.2	110.7	101.6	6.7
γ	−72.8	55.4	108.2	110.7	0.0[a]
ϵ	59.8	−140.1	110.0	106.1	6.9
		Axial α-Amino Group			
α	−59.1	−44.2	109.1	107.3	5.8
β	−178.2	−117.0	108.8	100.4	6.1
γ	−74.4	69.2	108.2	107.0	0.9

[a] Total energy = −898.6330 au.

TABLE 2: Selected Geometrical Parameters of the TOACDA Conformers Optimized at the PBE0/6-31G(d) Level[a]

	φ (deg)	ψ (deg)	α (deg)	τ (deg)	ΔE	ΔE (6-31+G(d,p)
			Equatorial α-Amino Group			
α	−71.4	−17.7	107.8	111.5	3.0 (1.1)	2.6
β	145.4	−150.8	110.7	101.8	7.0 (8.0)	7.2
γ	−73.7	55.8	107.8	110.5	0.0[b] (0.0[c])	0.0[d]
ϵ	59.3	−141.0	110.0	106.1	6.1 (3.2)	5.2
			Axial α-Amino Group			
α	−59.0	−44.4	109.1	107.5	5.6 (0.7)	5.8
β	−177.9	−116.1	108.7	100.5	6.1 (6.2)	6.0
γ	−75.0	70.5	108.0	106.8	1.0 (0.1)	1.2

[a] Using these geometries, relative stabilities (in kcal/mol) have been computed with both 6-31G(d) and 6-31+G(d,p) basis sets in vacuo and with the 6-31G(d) basis set also in aqueous solution (data in parentheses). [b] Total energy −898.7174 au. [c] Total energy −898.7396 au. [d] Total energy = −898.7792 au.

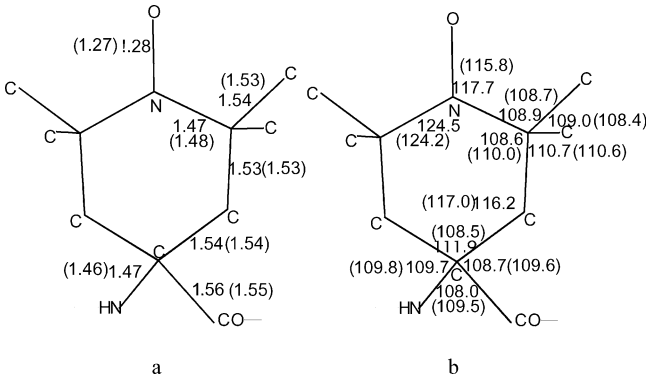

Figure 3. Comparison between geometrical parameters for the TOAC residue derived from the crystallographic analysis of peptides containing TOAC. Panel a shows experimental bond lengths (in Å), and panel b, experimental valence angles (in deg); the corresponding averages of the geometrical parameters computed for different conformers are reported in parentheses.

TABLE 3: Piperidine Ring Puckering for Different Conformers of TOACDA with an Equatorial α-Amino Group[a]

α	20% B	5% TB	75% C
β	37% B	61% TB	3% C
γ	23% B	1% TB	76% C
ϵ	21% B	76% TB	4% C

[a] The acronyms C, TB, and T refer to chair, twist-boat, and boat rings, respectively. (See the text for further details.)

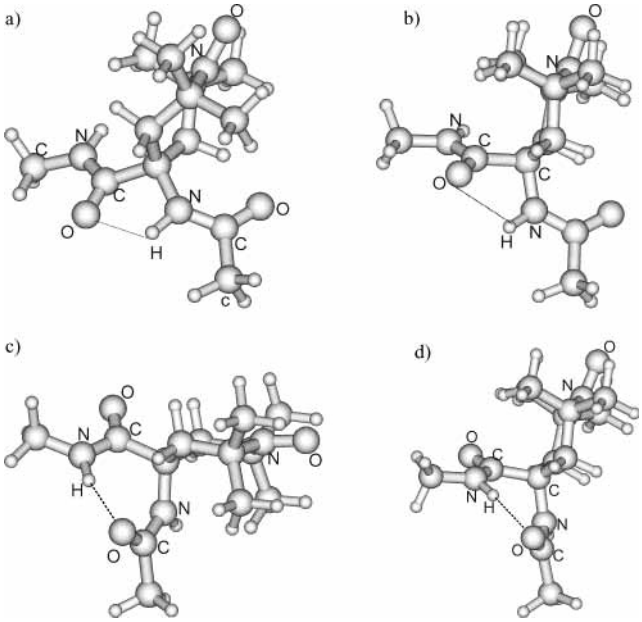

Figure 4. *β* and *γ* optimized structures for equatorial (a, c) and axial (b, d) placements of the α-amino group in the piperidine ring of TOAC dipeptide analogues.

but the piperidine ring of the other two conformers (*β* and *ϵ*) is intermediate between a twist and a boat (Table 3).

Helix structures of dipeptide analogues cannot form H bonds and are, therefore, significantly less stable, at least in the gas phase or in low-polarity solvents. As a consequence, *δ* conformers collapse in the high-energy α and *ϵ* minima shown in Figure 4 for both axial and equatorial placements of the α-amino group in the piperidine ring.

In summary, the relative stability of energy minima is *γ* > α > *ϵ* > *β* for the eq conformer and *γ* > α > *β* for the ax conformer. Note that the energy difference between *γ* and *β* structures is lower for an axial placement of the α-amino group because this situation allows the reduction of steric contacts with lower deformations of the piperidine ring. However, eq conformers are always more stable than their ax counterparts, the energy difference being ∼1.0 kcal/mol for the most stable *γ* structures. Crystallographic characterizations of peptides containing TOAC show that in the more populated piperidine ring conformation the α-amino and α-carboxy substituents occupy positions that are intermediate between the classical equatorial and axial positions.[9] This is in agreement with a low-energy difference between the limiting conformers, which can be easily modified to optimize crystal packing. It is significant that the insulated peptide derivative is characterized by two well-separated energy minima.

We have next analyzed the specific effects related to the presence of a nitroxide moiety on conformational equilibria. To this end, we have carried out calculations on the molecular system obtained by substituting the nitroxide group with $-CH_2$ in the piperidine ring (Table 4) and on the Ac_6c residue obtained

TABLE 4: Selected Geometrical Parameters and Relative Stabilities (kcal/mol) for the PBE0/6-31G(d) Energy Minima of the Amino Acid Derivative Obtained by Substituting the Nitroxide with a Methylene Group in the Piperidine Ring of TOAC

	φ (deg)	*ψ* (deg)	α (deg)	*τ* (deg)	Δ*E*
		Equatorial α-Amino Group			
α	−70.2	−19.4	107.8	111.5	2.8
β	159.1	−165.8	110.7	101.8	6.2
γ	−73.6	52.8	107.8	110.5	0.0[a]
ϵ	76.1	−59.5	110.0	106.1	2.5
		Axial α-Amino Group			
α	−57.7	−45	110.9	107.1	5.4
β	−177.8	−121.7	111.0	100.4	5.4
γ	−73.9	71.5	109.7	106.4	1.0

[a] Total energy = −808.2106 au.

TABLE 5: Selected Geometrical Parameters and Relative Stabilities (kcal/mol) for the PBE0/6-31G(d) Energy Minima of Ac_6cDA

	φ (deg)	*ψ* (deg)	α (deg)	*τ* (deg)	Δ*E*
		Equatorial α-Amino Group			
α	−68.8	−21.6	109.6	112.2	2.9
β	−167.8	−163.6	110.5	102.8	8.3
γ	−74.3	56.2	109.4	111.4	0.0[a]
ϵ	60.9	−145.1	109.6	107.4	10.2
		Axial α-Amino Group			
α	−63.1	−34.5	109.9	109.9	3.9
β	−178.9	−173.7	111.3	102.9	3.6
γ	−73.7	69.4	109.2	108.9	0.1

[a] Total energy = −651.1589 au.

TABLE 6: Selected Geometrical Parameters and Relative Stabilities (kcal/mol) for the PBE0/6-31G(d) Minima of AibDA in Vacuo and in Aqueous Solution[a]

	φ (deg)	*ψ* (deg)	α (deg)	*τ* (deg)	Δ*E*
α	−66.8	−25.2	110.3	112.1	2.9 (−0.5)
β	180	180	111.0	104.3	0.3 (−0.6)
γ	−73.8	57.2	109.8	111.8	0.0[b] (0.0[c])
δ	−174.7	33.9	110.8	108.0	4.4 (1.6)

[a] Data in parentheses. [b] Total energy = −534.5558 au. [c] Total energy = −534.5730 au.

by further replacing all of the methyl groups in positions 2 and 6 with hydrogen atoms (Table 5).

Our results show that methyl groups do not affect the general behavior of dipeptide analogues concerning both structural and energetic characteristics. The conformational behavior of all of the cyclic residues is quite similar but significantly different from that of the prototype C^{α}-tetrasubstituted amino acid residue Aib (Table 6), especially concerning the relative stability of the *β* conformer.

Both for TOAC and Ac_6c dipeptide analogues, the *β* conformer is characterized by a $NC^{\alpha}C'(\tau)$ valence angle that is considerably smaller than in other conformers, whereas the $C^{\beta}C^{\alpha}C^{\beta}(\alpha)$ angle is nearly constant and quite similar for different residues.

Note that for all cyclic residues both *β* and *ϵ* conformers are destabilized with respect to Aib, thus confirming that steric hindrances can be reduced only at the expense of significant ring distortions.

Several previous studies have shown that polar solvents can dramatically modify the relative stabilities of different conformers of peptides and that continuum solvent models usually provide reliable results.[22] In the case of TOACDA, free-energy calculations, performed in aqueous solutions for structures optimized in the gas phase, give the results collected in Table

TABLE 7: Relative Stabilities (kcal/mol) and Selected Geometrical Parameters of the Most Stable TOACDA Conformers in Aqueous Solution Optimized at the PCM/PBE0/6-31G (d) Level

	φ (deg)	ψ (deg)	α (deg)	τ (deg)	ΔE
		Equatorial α-Amino Group			
α	−70.1	−29.6	107.7	110.2	−0.2
γ	−75.1	57.2	107.6	109.8	0.0[a]
		Axial α-Amino Group			
α	−59.0	−44.4	109.1	107.5	0.8
γ	−75.0	70.5	108.0	106.8	1.0

[a] Total energy = −898.7410 au.

TABLE 8: Isotropic Hyperfine Coupling Constants (Gauss) of the Nitroxide Nitrogen Atom of TOACDA Calculated in Vacuo and in Aqueous Solution with the Composite Procedure of Equation 3[a]

	A_N (vacuum)	A_N (PCM)	A_N (PCM + $2H_2O$)
	Equatorial α-Amino Group		
α	14.72	15.31	16.83
β	12.35	13.17	14.31
γ	15.13	15.32	17.05
ϵ	12.61	12.93	14.63
	Axial α-Amino Group		
α	14.39	15.48	16.65
β	15.44	15.54	17.35
γ	15.39	15.70	17.28

[a] See the text for further details.

2. The general solvent effect is to reduce the stabilization induced by intramolecular hydrogen bonds due to their competition with intermolecular hydrogen bonds or, in macroscopic terms, due to the increase of the dielectric constant with the consequent reduction of the electrostatic attraction, which dominates the H-bond strength. As a consequence, the relative stability of helix structures is not far from that of γ conformers for both equatorial and axial placements of the α-amino group. However, β structures remain quite unstable because the solvent does not have a remarkable effect on steric hindrance. The effect of geometry reoptimization in solution was next investigated for the α and γ conformers. The results of Table 7 show a further slight stabilization of helical structures but confirm that, as previously reported,[22] geometries optimized in vacuo are sufficient for semiquantitative analyses.

Isotropic Hyperfine Couplings. We have computed the isotropic hyperfine couplings of all of the TOACDA conformers both in vacuo and in aqueous solution using the composite procedure described in the computational details. (See Table 8 for the essential results.)

The QCISD correction (second term on the right side of eq 3) is nearly constant (0.36 G) for all of the conformers and leads to A_N values that are in good agreement with the corresponding values measured in apolar solvents for related piperidine nitroxides.[21]

The most stable conformers (α and γ) of TOACDA show quite pyramidal nitroxide moieties, whereas the β and ϵ conformers are characterized by significantly lower hyperfine couplings and degrees of pyramidalization when the NO moiety occupies an equatorial position.

Because the singly occupied molecular orbital (SOMO) is mostly localized on the NO moiety (Figure 5), our results can be analyzed in terms of the competition between pyramidal (sp^3-like hybridization) and planar (sp^2-like hybridization) geometry around the nitrogen atom, which is tuned by the subtle balance of at least three different effects:

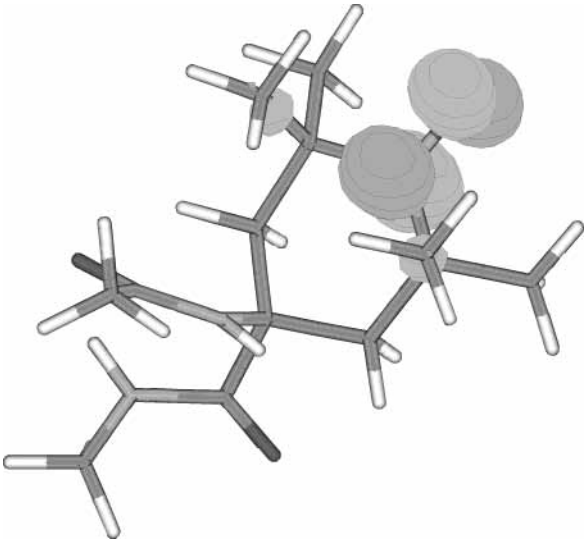

Figure 5. Singly occupied molecular orbital (SOMO) of TOACDA.

(1) the partial π bonding at the NO moiety, which favors sp^2 hybridization and thus planar geometry at the nitrogen atom;

(2) steric repulsions between the oxygen atom and the substituents on the α-carbon atom of the ring; and

(3) the stabilization (e.g., by polar solvents) of the resonance structure of nitroxides formally involving an N^+O^- moiety.

The neutral resonance structure with a lone pair on nitrogen is stabilized by a pyramidal environment, which minimizes the interelectronic repulsions; however, the N^+O^- resonance structure involves just one electron in the p-like orbital on nitrogen, and this favors planar geometry, which minimizes the repulsion among the three two-electron σ bonds of nitrogen.

When the nitrogen and its three substituents lie in the same plane, the SOMO is a pure π orbital, and the nitrogen atom lies in its nodal plane. As a consequence, the nominally unpaired orbital cannot give any direct contribution to hcc (delocalization term). However, the presence of an electron with unpaired spin (say, α) in the π system polarizes the electrons of the σ system and causes a slight excess of α electrons at the nitrogen nucleus: in a planar NO moiety, only this spin-polarization (indirect) effect contributes to A_N .

When the NO moiety is not perfectly planar, there is an increase in the s character of the SOMO, leading to some delocalization contribution to the hcc: the A_N value, then, increases remarkably.

Polar solvents stabilize the resonance structure involving charge separation, which implies an sp^2 hybridization of the nitrogen (planar geometry and bond angles closer to 120°). Therefore, a polar embedding medium, shifting some spin density from oxygen to nitrogen, increases A_N.

An experimental value is available for the A_N of a TOAC-labeled helical (3_{10}) lipopeptaibol in membranes.[38] Considering that A_N strongly depends on the environmental dielectric constant, we have performed some PCM computations using $CHCl_3$ and H_2O solvents. The A_N value computed in $CHCl_3$ solution (average value between eq and ax values of 15.2 G) is in fair agreement with experiment (15.4 G).[38]

The situation is more involved in aqueous solution because several studies have shown that the correct reproduction of solvent shifts induced by hydrogen-bonding solvents on the magnetic properties of polar solutes requires a balanced treatment of first-shell and bulk effects.[20,21] In particular, both experimental and QM results indicate that two water molecules are strongly bonded to the lone pairs of the nitroxide oxygen.

As a consequence, we have performed PCM computations both for the bare nitroxide and for the adduct containing two explicit water molecules (Figure 2). The results obtained by the latter discrete-continuum model (average A_N around 17 G, see Table 8) are in fair agreeement with experimental values for other six-membered ring nitroxides in aqueous solution (e.g., A_N = 17.1 G for 2,2,6,6-tetramethyl-4-carboxypiperidine nitroxide).[21c]

Conclusions

We have reported a detailed analysis of the structural and magnetic properties of a TOAC derivative both in vacuo and in aqueous solution. By analogy with natural amino acid residues, the global energy minimum falls in the γ region of the Ramachandran map, but the stability order of low-energy minima is quite peculiar. In particular, the β conformer is unusually unstable because of the steric hindrance of the piperidine ring, which can be relieved only by strong ring deformations. This behavior is retained when replacing the piperidine by a ciclohexane ring but changes significantly when α,α substitution does not involve a cyclic structure (Aib). Polar solvents modify the conformational behavior in a non-negligible way, stabilizing, in particular, helix structures. Concerning next the magnetic properties, our results are in remarkable agreement with the available experimental data and point out a number of interesting magneto−structural relationships. In particular, a significant tuning of hcc's by the backbone conformation has been evidenced, which is related to the different puckerings adopted by the piperidine ring to minimize steric repulsions.

The favorable scaling of our computational protocol with the dimensions of the system and its remarkable performances for both structural and magnetic properties pave the route for systematic studies of large polypeptidic systems involving the TOAC probe.

Acknowledgment. We thank Professor C.Toniolo (Padua University) for helpful discussions, Gaussian Inc. for financial support, and the Sezione di Modelistica Computazionale of the CIMCF (University Federico II) for computer facilities.

References and Notes

(1) Rassat, A.; Rey, P. *Bull. Soc. Chim. Fr.* **1967**, 815.
(2) Nakaie, C. L.; Goissis, G.; Schreirer, S.; Paiva, A. C. M. *Braz. J. Med. Biol. Res.* **1981**, *14*, 173.
(3) Marchetto, R.; Shreier, S.; Nakaie, C. R. *J. Am. Chem. Soc.* **1993**, *115*, 11042.
(4) Smythe, M. L.; Nakaie, C. R.; Marshall, G. R. *J. Am. Chem. Soc.* **1995**, *117*, 10555.
(5) Toniolo, C.; Crisma, M.; Formaggio, F. *Biopolymers* **1998**, *47*, 153.
(6) Pispisa, B.; Mazza, C.; Palleschi, A.; Stella, l.; Venanzi, M.; Formaggio, F.; Toniolo, C.; Broxterman, Q. B. *Biopolymers* **2002**, *67*, 247.
(7) Crisma, M.; Bianco, A.; Formaggio, F.; Toniolo, C.; Kamphuis, J. *Lett. Pept. Sci.* **1995**, *2*, 187.
(8) Bui, T. t. T.; Formaggio, F.; Crisma, M.; Torraca, V.; Toniolo, C.; Hussain, R.; Siligardi, G. *J. Chem. Soc., Perkin Trans.* **2000**, *2*, 1043.
(9) Toniolo, C.; Valente, E.; Formaggio, F.; Crisma, M.; Pilloni, G.; Corvaja, C.; Toffoletti, A.; Martinez, G. V.; Hanson, M. P.; Millhauser, G. L.; George, C.; Flippen-Anderson, J. L. *J. Pept. Sci.* **1995**, *1*, 45.
(10) Marshall, G. R. In *Intra-Science Chemical Reports*; Kharash, N., Ed.; Gordon and Breach: New York, 1971; pp 305−316.
(11) Karle, I. L.; Balaram, P. *Biochemistry* **1990**, *29*, 6747.
(12) Toniolo, C.; Benedetti, E. *Macromolecules* **1991**, *24*, 4004.
(13) Toniolo, C.; Crisma, M.; Formaggio, F.; Peggion, C. *Biopolymers* **2001**, *60*, 396.
(14) (a) Improta, R.; Barone, V.; Kudin, K. N.; Scuseria, G. E. *J. Am. Chem. Soc.* **2001**, *123*, 3311. (b) Improta, R.; Rega, N.; Aleman, C.; Barone, V. *Macromolecules* **2001**, *34*, 7550.
(15) Flippen-Anderson, J. L.; George, C.; Valle, G.; Valente, E.; Bianco, A.; Formaggio, F.; Crisma, M.; Toniolo, C. *Int. J. Pept. Protein Res.* **1996**, *47*, 231−238.
(16) Cornish, V. W.; Benson, D. R.; Altenbach, C. A.; Hideg, K.; Hubbel, W. L.; Scultz, P. G. *Proc. Natl. Acad. Sci. U.S.A.* **1994**, *91*, 2910−2914.
(17) Hanson, P.; Millhauser, G.; Formaggio, F.; Crisma, M.; Toniolo, C. *J. Am. Chem. Soc.* **1996**, *118*, 7618.
(18) Barone, V. In *Recent Advances in Density Functional Methods*; Chong, D. P., Ed.; World Scientific: Singapore, 1995; p 287.
(19) (a) Barone, V.; Bencini, A.; Di Matteo A. *J. Am. Chem. Soc.* **1997**, *119*, 10831. (b) Adamo, C.; Subra, R.; Di Matteo, A.; Barone, V. *J. Chem. Phys.* **1998**, *109*, 10244. (c) Barone, V.; Bencini, A.; Cossi, M.; Di Matteo, A.; Mattesini, M.; Totti, F. *J. Am. Chem. Soc.* **1998**, *120*, 7069. (d) Adamo, C.; Di Matteo, A.; Rey, P.; Barone V. *J. Phys. Chem. A* **1999**, *103*, 348. (e) Di Matteo, A.; Barone, V. *J. Phys. Chem. A* **1999**, *103*, 7676. (f) Di Matteo, A.; Adamo, C.; Cossi, M.; Barone, V.; Rey, P. *Chem. Phys. Lett.* **1999**, *310*, 159.
(20) (a) Improta, R.; Di Matteo, A.; Barone, V. *Theor. Chem. Acc.* **2000**, *104*, 273. (b) Improta, R.; Scalmani, G.; Barone, V. *Chem. Phys. Lett.* **2001**, *336*, 349.
(21) (a) Improta, R.; Kudin, K. N.; Scuseria, G. E.; Barone, V. *J. Am. Chem. Soc.* **2002**, *124*, 113. (b) Tedeschi, A. M.; D'Errico, G.; Busi, E.; Basosi, R.; Barone, V. *Phys. Chem. Chem. Phys.* **2002**, *4*, 2180. (c) Saracino, G. A. A. Tedeschi, A.; D'Errico, G.; Improta, R.; Franco, L.; Ruzzi, M.; Corvaia, C.; Barone, V. *J. Phys. Chem. A* **2002**, *106*, 10700.
(22) (a) Improta, R.; Benzi, C.; Barone, V. *J. Am. Chem. Soc.* **2001**, *123*, 12568. (b) Langella. E.; Improta, R.; Barone, V. *J. Am. Chem. Soc.* **2002**, *124*, 11531.
(23) Perdew, J. P.; Burke, K.; Ernzerhof, M. *Phys. Rev. Lett.* **1996**, *77*, 3685.
(24) Adamo, C.; Barone, V. *J. Chem. Phys.* **1999**, *110*, 6158.
(25) Frisch, M. J.; Trucks, G. W.; Schlegel, H. B.; Scuseria, G. E.; Robb, M. A.; Cheeseman, J. R.; Zakrzewski, V. G.; Montgomery, J. A., Jr.; Stratmann, R. E.; Burant, J. C.; Dapprich, S.; Millam, J. M.; Daniels, A. D.; Kudin, K. N.; Strain, M. C.; Farkas, O.; Tomasi, J.; Barone, V.; Mennucci, B.; Cossi, M.; Adamo, C.; Jaramillo, J.; Cammi, R.; Pomelli, C.; Ochterski, J.; Petersson, G. A.; Ayala, P. Y.; Morokuma, K.; Malick, D. K.; Rabuck, A. D.; Raghavachari, K.; Foresman, J. B.; Ortiz, J. V.; Cui, Q.; Baboul, A. G.; Clifford, S.; Cioslowski, J.; Stefanov, B. B.; Liu, G.; Liashenko, A.; Piskorz, P.; Komaromi, I.; Gomperts, R.; Martin, R. L.; Fox, D. J.; Keith, T.; Al-Laham, M. A.; Peng, C. Y.; Nanayakkara, A.; Challacombe, M.; Gill, P. M. W.; Johnson, B.; Chen, W.; Wong, M. W.; Andres, J. L.: Gonzalez, C.; Head-Gordon, M.; Replogle, E. S.; Pople, J. A. *Gaussian 99*, Development Version, revision A.03; Gaussian, Inc.: Pittsburgh, PA, 2000.
(26) *Exploring Chemistry with Electronic Structure Methods*, 2nd ed.; Foresman, J. B., Frisch, A. E., Eds.; Gaussian Inc.: Pittsburgh PA, 1996.
(27) Chipman, D. M. *Theor. Chim. Acta* **1989**, *76*, 73.
(28) Hariraran, P. C.; Pople, J. A. *Theor. Chim. Acta* **1973**, *23*, 213.
(29) (a) Weltener, W. *Magnetic Atoms and Molecules*; Dover: New York, 1989. (b) Barone, V.; Lelj, F.; Russo, N.; Ellinger, Y.; Subra, R. *Chem. Phys.* **1985**, *76*, 385.
(30) (a) Sekino, H.; Bartlett, R. J. *J. Chem. Phys.* **1985**, *82*, 4225. (b) Barone, V.; Grand, A.; Minichino, C.; Subra, R. *J. Phys. Chem.* **1993**, *97*, 6355. (c) Perera, S. A.; Salemi, L. N.; Bartlett, R. J. *J. Chem. Phys.* **1997**, *106*, 4061.
(31) Dapprich, S.; Komaroni, I.; Byun, K. S.; Morokuna, K.; Frisch, M. J. *J. Mol. Struct.: THEOCHEM* **1999**, *461*, 1.
(32) Cossi, M.; Scalmani, G.; Rega, N.; Barone, V. *J. Chem. Phys.* **2002**, *117*, 43.
(33) Scalmani, G.; Rega, N.; Cossi, M.; Barone, V. J. *Comput. Methods Sci. Eng.* **2002**, *2*, 159.
(34) Barone, V.; Cossi, M.; Tomasi, J. *J. Chem. Phys.* **1997**, *107*, 3210.
(35) Floris, F. M.; Tomasi, J. *J. Comput. Chem.* **1986**, *10*, 616.
(36) Pierotti, R. A. *Chem. Rev.* **1976**, *76*, 717.
(37) Cremer, D.; Pople, J. A. *J. Am. Chem. Soc.* **1975**, *97*, 1354.
(38) Monaco, V.; Formaggio, F.; Crisma, M.; Toniolo, C.; Hanson, P.; Milhauser, G. L. *Biopolymers* **1999**, *50*, 239.